

## Three-body recombination in two-dimensional atomic hydrogen gas

J. Järvinen, J. Ahokas, S. Jaakkola, and S. Vasilyev

*Wihuri Physical Laboratory, Department of Physics, University of Turku, 20014 Turku, Finland*

(Received 13 June 2005; published 16 November 2005)

We study three-body recombination in the gas of spin-polarized atomic hydrogen adsorbed on the surface of superfluid helium at temperatures from 45 to 130 mK. The two-dimensional gas is thermally compressed to densities up to  $\approx 4 \times 10^{12} \text{ cm}^{-2}$  using the “cold spot” method which makes the three-body process the dominant decay channel in the system. We measure the loss rate and surface density of atoms directly and independently and observe the former to be proportional to the third power of the latter. The result for the surface three-body recombination rate constant at 4.6 T,  $L_s = 2.0(7) \times 10^{-25} \text{ cm}^4/\text{s}$ , significantly reduces the discrepancy between the theory and earlier measurements where the surface density was inferred from the adsorption isotherm. We also measured the three-body rate constant on a 0.1%  $^3\text{He}$ - $^4\text{He}$  film and found  $L_s = 1.3(4) \times 10^{-24} \text{ cm}^4/\text{s}$ . This larger value is attributed to an increased delocalization of adsorbed hydrogen atoms in the direction normal to the surface.

DOI: [10.1103/PhysRevA.72.052713](https://doi.org/10.1103/PhysRevA.72.052713)

PACS number(s): 34.50.-s, 67.65.+z, 32.70.Jz, 76.60.Jx

### I. INTRODUCTION

Three-body recombination is an efficient tool to probe statistical correlations in quantum gases. It has been demonstrated in experiments with  $^{87}\text{Rb}$  [1,2] and two-dimensional (2D) spin-polarized atomic hydrogen [3] that appearance of a condensate in a Bose gas is accompanied by the reduction of the three-body recombination loss. On the other hand, three-body recombination appeared to be the most serious obstacle in achievement of high densities in the gas of spin-polarized hydrogen ( $\text{H}\downarrow$ ). Compression experiments of bulk  $\text{H}\downarrow$  have shown that this process may lead to a strong overheating of the sample cell surface or even to a thermal runaway [4–7]. Thus it has thwarted the achievement of Bose-Einstein condensate (BEC) in bulk  $\text{H}\downarrow$  gas confined by material walls. The values of the surface three-body recombination constant obtained in several measurements [4,5,8] are quite consistent with each other, but exceed the theoretical results of de Goeij *et al.* [9] by an order of magnitude.

Two methods of local compression have been utilized to reach quantum degeneracy in two-dimensional  $\text{H}\downarrow$  gas. The highest values of the quantum degeneracy parameter reached by magnetic compression [3] were  $\varpi = \sigma\Lambda^2 \approx 9$ . Here  $\sigma$  is the surface density and  $\Lambda$  is the thermal de Broglie wavelength. However, due to large field gradients, the magnetically compressed surface gas could not be studied directly. Thermal compression, known as the “cold spot” method, uses the enhanced adsorption of the  $\text{H}\downarrow$  gas at a colder surface. It does not require field gradients and allows a direct detection of the surface atoms by means of magnetic resonance. In our first experiments on the thermal compression of 2D  $\text{H}\downarrow$  [10] we attained  $\varpi \approx 1.5$ . We also estimated that the three-body recombination rate constant is at least an order of magnitude smaller than the values obtained in earlier indirect measurements [4,5,8]. The total recombination rate due to three-body recombination was found to be so small that we could not study it in detail. Thus it was not possible to conclude whether it is at all a limitation to the achievement of higher  $\varpi$  by the thermal compression techniques.

In the present work we eliminated most of the uncertainties to make accurate and reliable measurement of the surface three-body recombination rate constant. Electron-spin resonance [11] was used for direct detection of thermally compressed  $\text{H}\downarrow$  gas adsorbed on liquid helium. Three-body recombination was made the dominant density decay channel by increasing the size of the cold spot and reducing the rates of undesired one-body and two-body relaxation to a negligible level. We found the value  $L_s = 2.0(7) \times 10^{-25} \text{ cm}^4/\text{s}$  for the recombination rate constant at temperatures around 100 mK and revealed a weak temperature dependence of  $L_s$ . For  $\text{H}\downarrow$  adsorbed on  $^3\text{He}$ - $^4\text{He}$  mixture films we observed three-body recombination to be much faster with  $L_s = 1.3(4) \times 10^{-24} \text{ cm}^4/\text{s}$ . Our results are in fair agreement with the calculations of de Goeij *et al.* [9] bringing down the discrepancy between the theory and experiment. Finally, we discuss the limitations set by three-body recombination to the achievement of high quantum degeneracy by the thermal compression method.

### II. BACKGROUND

The loss rate  $R(t)$  of atoms due to their recombination into molecules is related to the density  $n$  of the gas confined in a volume  $V$  by [12]

$$\frac{1}{V}R(t) \equiv \frac{1}{V} \frac{dN}{dt} = -Gn - Kn^2 - Ln^3. \quad (1)$$

Here  $G$ ,  $K$ , and  $L$  are the first-, second-, and third-order loss rate constants, respectively, according to the number of atoms taking part in a single recombination or relaxation (with subsequent recombination) event. Recombination may occur in the bulk gas as well as on the sample cell walls, and the rate constants in Eq. (1) are in general sums of the surface and volume contributions. The loss rate due to the surface processes can be also expressed through the bulk density using the adsorption isotherm which in its classical limit reads

$$\sigma = n\Lambda \exp\left(\frac{E_a}{k_B T_s}\right) \quad (2)$$

with  $E_a$  being the adsorption energy and  $T_s$  the temperature of the adsorbed gas. Thus the total rate constant of three-body recombination may be expressed as

$$L = L_g + L_s^{eff}, \quad (3)$$

where the subscripts  $g$  and  $s$  correspond to the bulk and surface gas contributions, respectively. The effective surface recombination constant  $L_s^{eff}$  is related to the intrinsic rate constant  $L_s$  as

$$L_s^{eff} = L_s \frac{A}{V} \Lambda^3 \exp\left(\frac{3E_a}{k_B T_s}\right). \quad (4)$$

The three-body recombination loss rate appears to be about 3.8 times larger than the rate of three-body recombination events. According to calculations [9,13] the third atom taking part in the process will be depolarized (with  $\approx 0.9$  probability) and rapidly recombines in a subsequent collision with a fourth atom. Taking into account different possibilities for the final state of the third atom, each of the rate constants in Eqs. (3) and (4) can be written as  $L_{g,s} = L_{g,s}^{1/2} + L_{g,s}^{-1/2}$ , where the superscripts denote the spin projection of the third atom [9]. In experiments it has not been possible to study these decay channels separately. Therefore we prefer to use the term of the total recombination loss rate constant  $L_s$  rather than the event rate often denoted in literature as  $K_{bbb}$ .

In the three-body recombination mechanism described by Kagan *et al.* [13], the electronic dipole interactions in a collision of three H $\downarrow$  atoms induce a spin flip of one or two of the participating atoms. A molecule can be formed at the same time because of the presence of the third atom to satisfy the conservation laws. Therefore there is no principal difference for the process to occur in the bulk or on the surfaces of the experimental cell. The first calculation of the bulk rate constant  $L_g$  [13] agreed with the experiments [4,5,7,8]. To estimate the surface rate constant it was pointed out [14] that for low values of adsorption energy,  $E_a \lesssim 1$  K, the delocalization of the adsorbed atoms in the direction perpendicular to the surface given by  $l = \hbar / (2mE_a)^{1/2}$  may become larger than the characteristic radius  $r_0$  of the interaction potential of the atoms ( $\approx 0.35$  nm for H $\downarrow$  in three dimensions). In this case interatomic collisions may be treated as three dimensional, and the rate constant of the surface recombination is related to the bulk one as [14,15]  $L_s \approx L_g / l^2$ . The value  $L_s \approx 2 \times 10^{-24}$  cm<sup>4</sup>/s estimated on the basis of such a scaling approach agrees roughly with the measurements [4,5,8]. However, more elaborate calculations [9,16], the former of which takes into account the actual profile of the atomic wave function in the perpendicular direction, give nearly an order of magnitude smaller values in the 5–10-T range. Furthermore, the calculations predict a field dependence that is in qualitative disagreement with experiments in this range (opposite sign, for both bulk and surface processes). At very high magnetic fields (10–20 T), the situation reverses and the calculations all predict the qualitative field dependence measured by the experiment [7]. The cal-

culations from the two independent groups and the experiment all converge in absolute value at the highest field measured to date [7].

The bulk density  $n$  was typically the main and most easily accessible quantity measured as a function of time during the decay of a H $\downarrow$  sample. The observed  $n(t)$  was fitted to the rate equation (1) with the effective rate constants being free parameters. Then, the intrinsic surface recombination rate and  $E_a$  were obtained, respectively, as the intercept and the slope of the plots of the logarithm of the effective rate vs  $1/T_s$  [cf. Eq. (4)]. However, such an approach may lead to errors if there are undetected temperature inhomogeneities.

### III. EXPERIMENT

The first estimate of the three-body recombination constant based on independent measurements of the surface density and the recombination loss rate was reported in our previous work [10] where 2D H $\downarrow$  gas was compressed thermally on a cold spot (CS) of 0.15 cm diameter located in the center of an (electron spin resonance) ESR resonator. The surface of the CS is oriented perpendicular to the main polarizing field. This sidesteps complications related with two-body dipolar relaxation on the surface as it is known that the rate of this process vanishes in such an orientation [17]. The CS was actively cooled by the <sup>3</sup>He-<sup>4</sup>He mixture of a dilution refrigerator to a constant temperature in the range 50–100 mK, while the rest of the sample cell (SC) walls were kept at a somewhat higher temperature. Being aware of three-body recombination on the CS, we made the latter to have a relatively small area. It turned out, however, that the contribution of the cold spot to the atom loss was hardly discernible from the background of the one-body relaxation rate. Using special techniques of rapidly activating or deactivating the thermal compression we could detect a small increase of the recombination heat appearing due to the high density on the cold spot. We were able to estimate roughly that the three-body recombination rate constant is at least an order of magnitude smaller than was expected. Quantitative studies of the recombination processes in the dense 2D H $\downarrow$  gas were not possible due to the too small size of the compression region. Having the size of the cold spot smaller than the waist of the mm-wave beam in the resonator leads to another difficulty related with an inhomogeneous density profile near the spot edge. This caused an inhomogeneous broadening of the ESR lines which made it impossible to study the broadening due to interactions in the 2D gas.

For the present work we redesigned the sample cell including the ESR resonator and the cold spot (Fig. 1). The diameter of the cold spot was increased to 0.6 cm. At the same time the thermal isolation of the cold spot from the cell walls was improved by connecting them with a 20- $\mu$ m Mylar foil. The volume of the sample cell was increased to 40 cm<sup>3</sup> thus eliminating the need for a buffer volume used previously [10,18]. To reduce the rate of undesirable one-body relaxation we covered most of the inner sample cell walls with a 20- $\mu$ m Mylar foil glued with Stycast 1266 epoxy [19]. A further decrease of the relaxation rate was obtained by coating the walls with a H<sub>2</sub> layer. A hydraulic valve

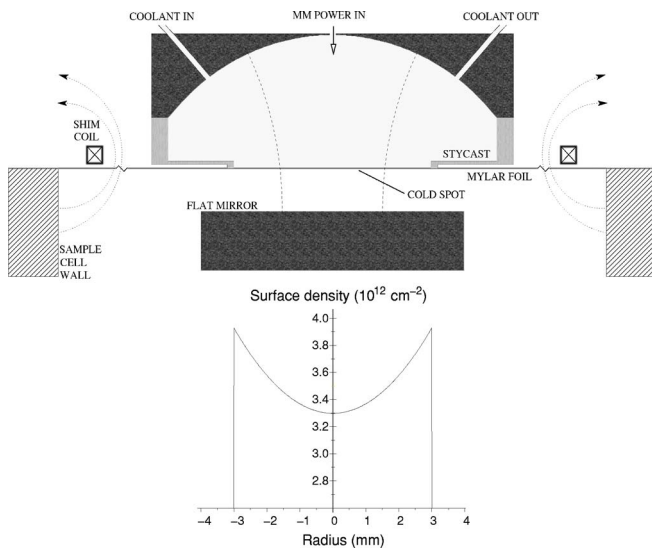


FIG. 1. (Color online) Schematic drawing of the Fabry-Perot ESR resonator with the cold spot. The graph shows a calculated density profile for high surface densities,  $\sigma \gtrsim 3.3 \times 10^{12} \text{ cm}^{-2}$ , obtained by optimizing the shim coil current for narrowest linewidth.

based on the fountain effect in superfluid  $^4\text{He}$  was installed in the  $\text{H}\downarrow$  filling line between the sample cell and a cryogenic dissociator.

In a typical measurement we first load the sample cell with  $\text{H}\downarrow$  gas from the dissociator. After the sample accumulation we turn off the dissociator, close the fountain valve at the SC inlet, and cool the SC down to a desired temperature in the range  $T_c = 120\text{--}200$  mK. The temperatures of the mixing chamber of the dilution refrigerator, the cold spot cooling mixture ( $T_m$ ), and the sample cell are actively stabilized during the measurement of the decay. The thermal link between the SC and mixing chamber is strong enough to remove recombination heat of the order  $10 \mu\text{W}$  but yet allows a sensitive measurement of this heat. The bulk gas in the SC and the 2D gas on the cold spot are detected by ESR at 128 GHz [11,18]. During the sample accumulation we can detect the ESR lines of the hyperfine transitions  $a \rightarrow d$  and  $b \rightarrow c$ , but rapidly after turning off the dissociator the first line disappears due to preferential recombination of the “mixed”  $a$  state which makes the sample doubly polarized in the “pure”  $b$  state. A typical collection of experimental data obtained during the decay of the  $\text{H}\downarrow$  sample includes a set of ESR  $b \rightarrow c$ -transition spectra of bulk and 2D atoms and the feedback power of the SC temperature controller as a function of time. The bulk gas density  $n$  is extracted from the integral of the corresponding ESR lines. To calculate surface density  $\sigma$  from the ESR spectra we use the shift  $\Delta B$  of the surface line from the bulk one. It has been shown in our previous work [10,18] that the shift depends linearly on the surface density as  $\Delta B = 1.0(1) \times 10^{-12} \text{ cm}^2 \times \sigma$ . The recombination loss rate  $R(t)$  is calculated from the feedback power of the SC temperature controller. By integrating  $R(t)$  we get an independent method to measure the bulk density, also used for its absolute calibration.

The 2D ESR line shapes observed in the present work are narrow and symmetrical, with the width increasing lin-

early with the surface density from 0.1 to 0.15 G, up to  $\sigma \approx 3.3 \times 10^{12} \text{ cm}^{-2}$ . At higher densities the lines broaden rapidly to 0.5 G and become asymmetrical. Contrary to the previous measurements [10] we did not observe any influence of the temperature difference between the SC and CS on the line shapes of the surface atoms. The minimum observed width of 0.1 G, interpreted as our instrumental linewidth, may be caused by the frequency instability of the mm-wave source or a pickup current in the magnetic-field sweep coil. The reasons for the changes of the line shape and its broadening at  $\sigma \gtrsim 3.3 \times 10^{12} \text{ cm}^{-2}$  are not clear at present. A possible reason is that recombination overheating leads to an inhomogeneity of the temperature and surface density on the cold spot. In this work we use data for smaller surface densities only where the lines do not exhibit inhomogeneous broadening.

## IV. RESULTS

### A. Pure $^4\text{He}$ surface

In Fig. 2 we present data obtained during several  $\text{H}\downarrow$  decays at the sample cell temperature  $T_c = 178$  mK and various cold spot temperatures. At a high cold spot temperature like 160 mK the decay is of first order, governed by  $b \rightarrow a$  relaxation on the sample cell walls. The rate constant of this process was minimized to  $G_s \approx 8 \times 10^{-2} \text{ s}^{-1}$  by coating the cell walls with a  $\approx 30$ -nm-thick  $\text{H}_2$  film. When lowering the sample cell temperature to about 100 mK the decay deviates from the first-order character indicating that some higher-order processes start to appear. The  $\text{H}\downarrow$  surface density on the sample cell walls was not known, making the analysis of the decays for low  $T_c$  difficult. Therefore we kept the SC temperature relatively high, e.g., at  $T_c = 178$  mK, where we could still achieve surface densities on the cold spot close to the maximum possible in this setup. We run a series of decays with different temperatures  $T_m$  of the  $^3\text{He}$ - $^4\text{He}$  liquid cooling the cold spot. Decreasing the cold spot temperature increases the recombination rate which is clearly visible from the rate of change of the bulk density [Fig. 2(a)] as well as from the total loss rate independently calculated from the recombination power [Fig. 2(b)]. Due to recombination overheating the temperature  $T_s$  of the 2D gas on the cold spot at high surface densities differs from  $T_m$ . To find  $T_s$  we use the adsorption isotherm [Eq. (2)], which method works very well since we measure the surface and bulk densities independently [10].

Raising the cold spot temperature to above  $\sim 150$  mK does not influence any more the decay rate in the sample cell, which we then define as background cell contribution  $R_c(n)$  [lowermost trace in Fig. 2(b)]. To find the contribution of the cold spot to the decay we subtract  $R_c(n)$  from the rates measured at lower temperatures of the cold spot. In Fig. 3(a) we plot this difference  $R_s$  as a function of the third power of the surface density,  $\sigma_s^3$ . Unfortunately, due to the recombination overheating the temperature of the 2D gas does not remain constant, as can be seen from Fig. 3(b). However, these relatively small changes do not influence the recombination loss rate significantly, since the points with different  $T_s$  fall roughly on the same line in Fig. 3(a). The linearity of the  $R_s$  vs  $\sigma_s^3$  plot proves that we are dealing with third-order recom-

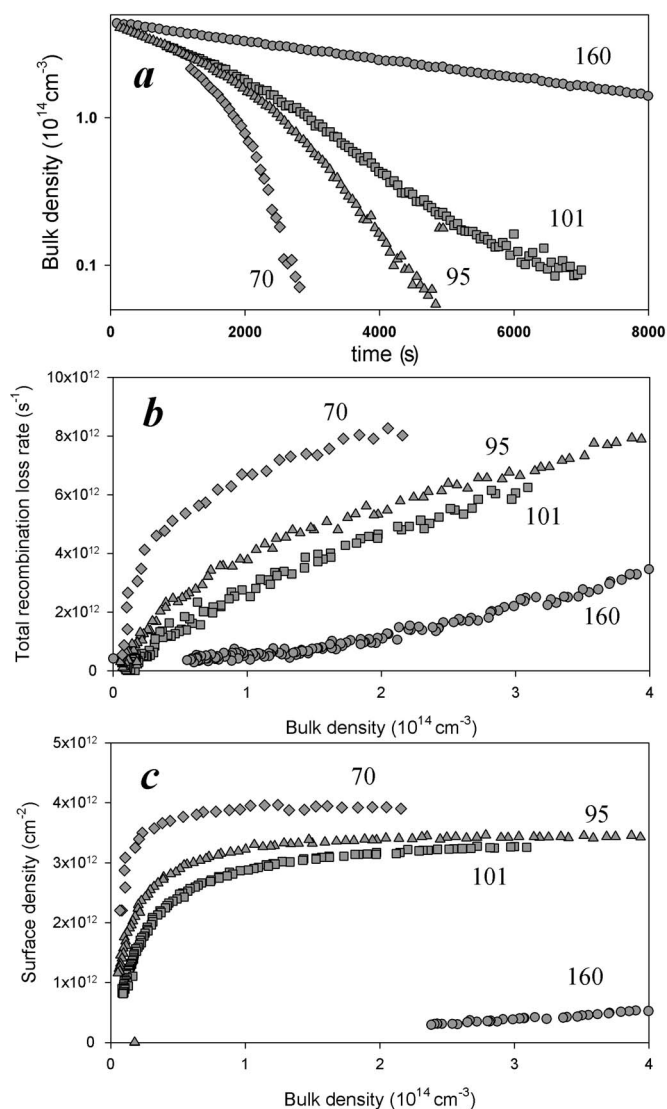


FIG. 2. Typical set of data obtained during decays of hydrogen sample at cell temperature  $T_c=178$  mK and various temperatures  $T_m=160$  mK ( $\bullet$ ), 101 mK ( $\blacksquare$ ), 95 mK ( $\blacktriangle$ ), and 70 mK ( $\blacklozenge$ ) of the cold spot coolant mixture.

bination described by the simple equation  $R=L_3\sigma_s^3A_s$ . Then, the rate constant is found from the slope of the line fitted to the data of Fig. 3. For the area of the cold spot  $A_s$  we take its geometrical area  $0.32 \text{ cm}^2$ . The region where we can detect 2D  $\text{H}\downarrow$  is defined by the  $\approx 0.3$ -cm-diameter waist of the mm-wave beam in the resonator. Therefore we cannot detect atoms close to the edge of the cold spot. In our previous cell [10] the beam waist was larger than the cold spot and by numerical processing of the ESR spectra we were able to restore the density profile near the spot edge. It turned out that the density profile has a rather steep step at the edge, so that three-body recombination outside the spot was estimated to be negligibly small. The improved thermal insulation of the cold spot region in the present setup, together with the larger size of the spot, makes the step approximation of the surface density even better and justifies the use of the geometrical area in the determination of the absolute value of the rate constant.

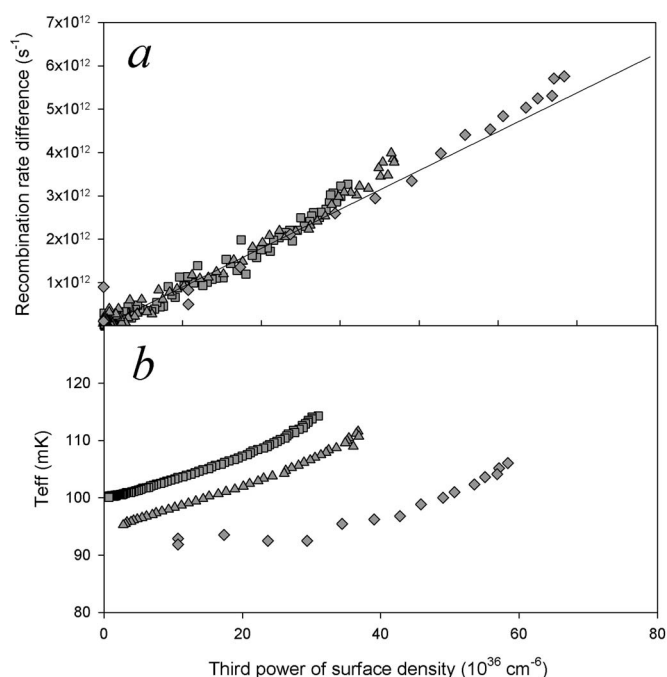


FIG. 3. (a) Recombination loss rate and (b) temperature of the 2D gas at the cold spot at cell temperature  $T_c=178$  mK and different temperatures of the cold spot  $T_s=101$  mK ( $\blacksquare$ ), 95 mK ( $\blacktriangle$ ), and 70 mK ( $\blacklozenge$ ).

A small nonlinearity of the  $R(\sigma_s^3)$  plot can be caused by temperature changes in the surface gas during the decay. To elucidate a possible temperature dependence we calculate the rate constant  $L_s$  as the ratio  $R_s/\sigma_s^3A_s$  for each data point and plot it as a function of  $T_s$  in Fig. 3.

Unfortunately,  $\sigma_s(T_s)$  decreases rapidly with increasing  $T_s$  following the adsorption isotherm (2). This limited the maximum temperature at which we could obtain useful data to about 120 mK. To get some data for higher temperatures (the 130-mK point in Fig. 4), we used the method of rapid switching the thermal compression on/off as described in our previous work [10].

### B. $^3\text{He}$ - $^4\text{He}$ mixture films

It is known that the presence of even a small amount of  $^3\text{He}$  in liquid  $^4\text{He}$  strongly influences the adsorption energy of  $\text{H}\downarrow$  [20]. We added 0.1 at. % of  $^3\text{He}$  into  $^4\text{He}$  and run similar decays as with isotopically pure  $^4\text{He}$ . According to the measurements of Safonov *et al.* [20] this concentration will reduce the adsorption energy to  $\approx 0.5$  K. Because the surface density scales as  $\exp(E_a/T_s)$ , we expected that a decrease of temperature by a factor of  $\approx 2$  would lead to the same values of surface densities and decay rates as for pure  $^4\text{He}$ . Indeed, the value of the one-body relaxation rate constant at  $T_c=88$  mK appeared to be about the same as with pure  $^4\text{He}$  at  $T_c=178$  mK. But the surface density at the cold spot appeared to be significantly smaller even at the lowest spot coolant temperature of 45 mK. We could not compress the 2D  $\text{H}\downarrow$  samples to surface densities higher than  $10^{12} \text{ cm}^{-2}$  on the mixture film. Knowing both densities  $\sigma$  and  $n$ , we

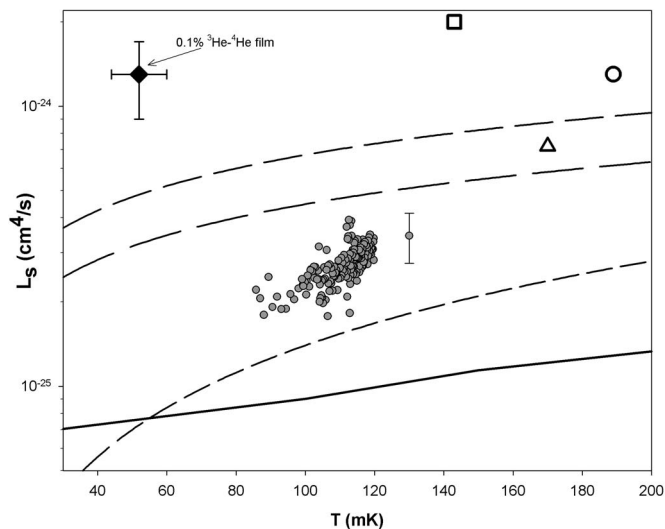


FIG. 4. Summary of data for the three-body recombination rate constant  $L_s$ . Closed circles represent data obtained in this work at various temperatures of the 2D gas using pure  $^4\text{He}$ , diamond stands for 0.1%  $^3\text{He}$ - $^4\text{He}$  mixture film. Dashed lines are the extrapolations of the results of Bell *et al.* [5] with certain assumed temperature dependencies (see text for explanation).  $\circ$ : Sprik *et al.* [4];  $\square$ : Reynolds *et al.* [8];  $\triangle$ : Safonov *et al.* [3]. Solid line is calculation of de Goey *et al.* at 4.6-T field.

calculated the ratio  $E_a/T$  and found that it does not remain constant during the decay. This may be explained by changes of the adsorption energy or the surface temperature. The latter seems to be more feasible, since the heat transfer from the adsorbed gas to helium is mediated by a poor thermal contact between riplons and phonons of the film [21] which scales as  $T^{20/3}$  and is expected to be a most serious obstacle of cooling the surface gas substantially below 100 mK. Lowering the film temperature by a factor of 2 leads to a decrease in heat conductance by two orders of magnitude. Although we failed in the compression of the surface gas to high densities, the influence of the cold spot on the decay kinetics was well visible (Fig. 5). After the same data processing as for pure  $^4\text{He}$ , we plot the contribution of the cold spot to the recombination rate as a function of the third power of surface density [Fig. 5(b)]. Fitting a line to the data yields the value  $L_s = 1.3(4) \times 10^{-24} \text{ cm}^4/\text{s}$  for the three-body rate constant. Assuming that during the decay the adsorption energy remains constant at  $E_a = 0.5 \text{ K}$  we estimate that the surface temperature on the cold spot is changing from 60 to 45 mK. This defines the error bar for the corresponding point in Fig. 4.

### C. Sources of error

One of the possible errors in the determination of  $L_s$  in our experiments comes from the uncertainty in the  $\text{H}\downarrow$  surface density profile over the cold spot region. As mentioned above, at high surface densities,  $\sigma = 3.3\text{--}4 \times 10^{12} \text{ cm}^{-2}$ , we observed broadening of the ESR lines. From the previous work [10] we know that inhomogeneous surface density can cause density dependent broadening. To verify this, we ap-

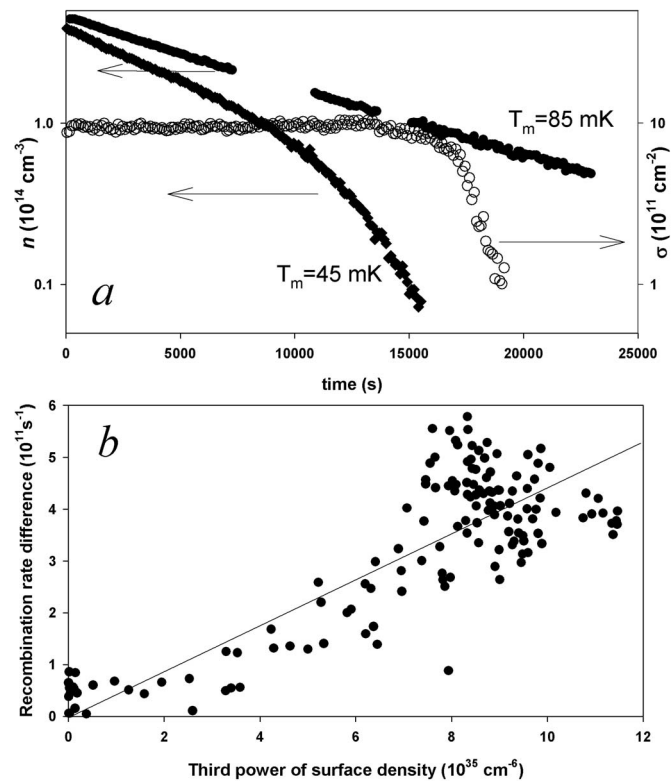


FIG. 5. Experimental data obtained from the decays with 0.1% mixture  $^3\text{He}$ - $^4\text{He}$  film at the sample cell temperature  $T_c = 88 \text{ mK}$ . (a) Evolution of bulk density at  $T_m = 85 \text{ mK}$  ( $\bullet$ ) and  $T_m = 45 \text{ mK}$  ( $\blacklozenge$ ), and of surface density at  $T_m = 45 \text{ mK}$  ( $\circ$ ). (b) Recombination rate on the cold spot at  $T_m = 45 \text{ mK}$  as a function of the third power of surface density. Solid line is a linear fit to the data with  $L_s = 1.3(4) \times 10^{-24} \text{ cm}^4/\text{s}$ .

plied an extra magnetic field with parabolic radial profile of a miniature shim coil mounted to the sample cell (Fig. 1). By changing the strength and direction of the current we found that the broadening can be partially explained by the density profile with the surface density increasing towards the edge of the cold spot. We consider the recombination overheating of the surface gas as the main reason for such a density profile. Excited  $\text{H}_2$  molecules, escaping from the 0.1-cm gap between the cold spot and the flat mirror of the ESR resonator (Fig. 1), experience on the average a larger number of collisions with the central regions of the spot than with its edge. Our simulations of this process show that it may lead to a heat flux to the surface which decreases parabolically towards the edge of the spot. By minimizing the linewidth with the shim coil we can estimate the field and hence the density profiles appearing in the central region of the cold spot with  $\rho \leq 0.15 \text{ cm}$ . For the surface density in the spot center  $\sigma_s(0) = 3.3 \times 10^{12} \text{ cm}^{-2}$  we find that the radial density distribution is represented by the function  $\sigma_s(\rho) \approx (3.3 + 7\rho^2) \times 10^{12} \text{ cm}^{-2}$  ( $\rho$  in cm), plotted in Fig. 1. We extrapolate this density profile to the edge of the spot and calculate the three-body recombination loss rate by integrating  $L_s \sigma_s(\rho)^3$  over the spot area. For the integrated rate we obtain  $\approx 35\%$  larger value than the simple geometrical value of  $L_s \sigma_s(0)^3 A_s$ . This may lead to overestimation of  $L_s$  by the

same amount, and the error should be much smaller for the lower density points where the effect of the density profile vanishes.

Another error may arise from the inaccuracy of the calibration of the surface density vs the shift  $\Delta B$  of the 2D ESR line from the bulk line. The measurement of the shift is straightforward with an accuracy better than the half width of the lines ( $\approx 80$  mG). In the considered density range this leads to an error of at most 5%. For the calibration of the surface density we compare the area under the surface absorption line shape with that of the bulk line. A quantity involved in the calibration procedure is the ratio of integrals of the mm-wave  $H_1$  field over the volume of the bulk sample and the area of the adsorbed gas. The presence of dielectric materials like epoxy and liquid helium in the resonator complicates the calculation of the ratio. We estimate the calculation to be accurate to within 10%, which leads to the same error in the calibration of the shift  $\Delta B$  against  $\sigma$ , used to calculate surface density. Finally, we estimate that the sources of error mentioned above may lead to an overall 30% error in the determination of the three-body rate constant  $L_s$ .

## V. DISCUSSION

To compare our results with those obtained in earlier H $\downarrow$  measurements, we have to take into account the different experimental conditions (magnetic field and temperature range) in which the measurements have been carried out. The results reported for the three-body surface recombination rate constant in Refs. [3–5,8] are summarized in Fig. 4. Bell *et al.* [5] and Sprik *et al.* [4] report a small decrease of the rate constant with increasing magnetic field  $B$  which is, however, in disagreement with the theory of de Goey *et al.* [9] who predict a growth of  $L_s(B)$  in the range of the fields considered. The field dependence has been observed to reverse, however, at higher magnetic fields [7], and only comes into full quantitative agreement with calculations at 20 T, after yet a second reversal. The comparison of data and calculations taken at different fields in the 5–10-T range therefore remains problematic. The calculated result [9] for the temperature variation of  $L_s$  in the present field  $B=4.6$  T are plotted with a bold solid line in Fig. 4. One can see that our data lie substantially below the previous experiments, but still above the theoretical value. The weak temperature dependence of  $L_s$  indicated by our data may be explained by the increase of the ternary collision rate at higher temperatures and agrees with the calculations [9]. The much larger values of  $L_s$  obtained in the previous measurements may be accounted for on the basis of an underestimation of the value of the adsorption energy used in the processing of the data. The surface recombination rate constant was calculated from the effective bulk rate using Eq. (4) with  $E_a$  extracted from the fit of  $L_s^{eff}$  vs  $1/T$ . Bell *et al.* [5], who made decay measurements down to 250 mK only, varied the value of  $E_a$  and included some hypothetical temperature dependencies of  $L_3$  in their fits, which we extrapolate in Fig. 4 to below 250 mK. The uppermost of the dashed lines stands for  $E_a=0.99$  K and  $L_s$

$=1.5 \times 10^{-24} \times (T/0.5 \text{ K})^{1/2}$ , the middle line for  $E_a=1.08$  K and  $L_s=1.0 \times 10^{-24} \times (T/0.5 \text{ K})^{1/2}$ , and the lower one for  $E_a=1.15$  K and  $L_s=7.0 \times 10^{-25} \times (T/0.5 \text{ K})$ . Due to the strong exponential factor in Eq. (3) such relatively small changes of  $E_a$  lead to rather large differences in  $L_s$ . Sprik *et al.* and Reynolds *et al.* extracted their results from the fits with  $E_a$  fixed to 1.0 K. If we recalculate  $L_s$  from their data by using the latest value  $E_a=1.14$  K [20], we get an order of magnitude smaller values which agree well with our results. In Fig. 4 we present also the value of  $L_s$  obtained in our magnetic compression experiments [3], where the value  $E_a=1.01$  K was used.

We found an eightfold increase of the three-body recombination rate constant on the mixture  $^3\text{He}$ - $^4\text{He}$  films. The most important difference of the mixture from the pure  $^4\text{He}$  film is that  $^3\text{He}$  may, like atomic hydrogen, occupy the surface bound states. This influences the surface interaction potential for hydrogen making it more diffusive and results in a substantial decrease of the adsorption energy [20]. A smaller value of the adsorption energy leads to a larger size  $l$  of the atomic wave function in the direction  $z$  perpendicular to the surface. According to de Goey *et al.* [9]  $L_s$  is sensitive to the shape and width of the wave function in the  $z$  direction. The authors [9] use the function of the shape  $\phi_0=2l^{-3/2}z \exp(-z/l)$  with  $l=0.37$  nm. Kagan *et al.* [14] used a somewhat broader function,  $\tilde{\phi}_0=(2/l)^{1/2} \exp(-z/l)$  with  $l=0.53$  nm, and got a factor of 2.4 larger value for  $L_s$ . Such a dependence on the delocalization length  $l$  agrees with our result for  $L_s$  on  $^3\text{He}$ - $^4\text{He}$  films with  $E_a=0.5$  K for which  $l$  is about 1.5 times larger than for pure  $^4\text{He}$  film. However, this is in contradiction with the scaling approach described in Refs. [14,15], according to which the surface rate constant should be related to the bulk one as  $L_s \sim L_g/l^2$ . One should bear in mind that the validity of the scaling approach is justified by the inequality  $l \gg r_0$ , which is not fulfilled for the case of atomic hydrogen where we rather have  $l \sim r_0$ . Knowing the correct dependence of  $L_s$  on  $E_a$  would be important also from the viewpoint of reaching higher degeneracies in 2D H $\downarrow$ .

The maximum values of quantum degeneracy of  $\varpi \approx 1.5$  that can be reached in thermal compression experiments (present work and Ref. [10]) are limited by overheating of the surface gas due to three-body recombination in the compression region. The heat flux through the surface due to this process increases rapidly with the surface density as  $Q_{rec}=L_s\sigma^3 fD$ , where  $D=3.7 \times 10^{-19}$  J is the dissociation energy per atom and  $f \approx 0.01$  is the fraction of the recombination energy deposited into the film at the recombination site [22]. This heat flux cannot exceed the maximum cooling power of the surface  $Q_{cool}=G_{rp}T_s^{20/3}$  dictated by the thermal contact  $G_{rp}$  between ripplons and phonons of the film [21]. If we neglect all other sources of heat to the surface, we obtain

$$\varpi_{max} = \frac{2\pi\hbar^2}{mk_b} \left( \frac{G_{rp}}{DL_s f} \right)^{1/3} T_s^{11/9}. \quad (5)$$

The influence of  $L_s$ ,  $f$ , and  $G_{rp}$  on  $\varpi_{max}$  is rather weak as defined by the third-power dependence of the recombination rate on  $\sigma$ . Evaluating  $\varpi_{max}$  from Eq. (5) we get

$\varpi_{\max} \approx 30 \text{ K}^{-11/9} \times T_s^{11/9}$ . For  $T_s=0.1 \text{ K}$  this gives  $\varpi_{\max} \approx 1.8$ , in good agreement with the values achieved in the experiments. According to Eq. (5) increasing the surface temperature would help to get a higher degeneracy, but then the surface density would decrease according to Eq. (2) and one would need much higher bulk densities to retain the same  $\sigma$ . This problem may be solved with a more intense  $\text{H}_2$  source or by compressing the bulk gas. On the other hand, an increase in the bulk density is limited by the growth of the heat flux to the cold spot due to thermal accommodation of the bulk atoms. We estimate that at densities  $n = 10^{15} - 10^{16} \text{ cm}^{-3}$  and surface temperatures  $T_s \approx 150 \text{ mK}$  one may reach the quantum degeneracy  $\varpi \approx 2.5$ . Another way to work at higher surface temperatures would be to increase

simultaneously the adsorption energy. This can be done by utilizing thin unsaturated films of  $^4\text{He}$  [23]. In this case one may also hope that the three-body recombination rate constant will decrease because of the smaller delocalization length  $l$  of the adsorbed atoms.

#### ACKNOWLEDGMENTS

We wish to thank Kalle-Antti Suominen for illuminating discussions. J.J. wishes to thank also the National Graduate School in Materials Physics for financial support. This work was supported by the Academy of Finland (Grant Nos. 78149 and 206109) and the Wihuri Foundation.

- 
- [1] E. A. Burt, R. W. Ghrist, C. J. Myatt, M. J. Holland, E. A. Cornell, and C. E. Wieman, *Phys. Rev. Lett.* **79**, 337 (1997).
- [2] B. L. Tolra, K. M. O'Hara, J. H. Huckans, W. D. Phillips, S. L. Rolston, and J. V. Porto, *Phys. Rev. Lett.* **92**, 190401 (2004).
- [3] A. I. Safonov, S. A. Vasilyev, I. S. Yasnikov, I. I. Lukashevich, and S. Jaakkola, *Phys. Rev. Lett.* **81**, 4545 (1998).
- [4] R. Sprik, J. T. M. Walraven, G. H. van Yperen, and I. F. Silvera, *Phys. Rev. B* **34**, 6172 (1986).
- [5] D. A. Bell, H. F. Hess, G. P. Kochanski, S. Buchman, L. Pollack, Y. M. Xiao, D. Kleppner, and T. J. Greytak, *Phys. Rev. B* **34**, 7670 (1986).
- [6] T. Tommila, S. Jaakkola, M. Krusius, I. Krylov, and E. Tjukanov, *Phys. Rev. Lett.* **56**, 941 (1986).
- [7] J. D. Gillaspay, I. F. Silvera, and J. S. Brooks, *Phys. Rev. B* **40**, 210 (1989).
- [8] M. W. Reynolds, I. Shinkoda, W. N. Hardy, A. J. Berlinsky, F. Bridges, and B. W. Statt, *Phys. Rev. B* **31**, 7503 (1985).
- [9] L. P. de Goey, H. T. C. Stoof, J. M. Vianney, A. Koelman, B. J. Verhaar, and J. T. M. Walraven, *Phys. Rev. B* **38**, 11500 (1988).
- [10] S. Vasilyev, J. Järvinen, A. I. Safonov, and S. Jaakkola, *Phys. Rev. A* **69**, 023610 (2004).
- [11] S. Vasilyev, J. Järvinen, E. Tjukanoff, A. Kharitonov, and S. Jaakkola, *Rev. Sci. Instrum.* **75**, 94 (2004).
- [12] I. F. Silvera and J. T. M. Walraven, *Progress in Low Temperature Physics*, edited by D. F. Brewer (North-Holland, Amsterdam, 1986), Vol. X.
- [13] Y. Kagan, I. A. Vartanyantz, and G. V. Shlyapnikov, *Zh. Eksp. Teor. Fiz.* **81**, 1113 (1981) [*Sov. Phys. JETP* **54**, 590 (1981)].
- [14] Y. Kagan, G. V. Shlyapnikov, I. A. Vartanyantz, and N. A. Glukhov, *Pis'ma Zh. Eksp. Teor. Fiz.* **35**, 386 (1982) [*JETP Lett.* **35**, 477 (1982)].
- [15] D. S. Petrov, M. Holzmann, and G. V. Shlyapnikov, *Phys. Rev. Lett.* **84**, 2551 (2000).
- [16] H. T. C. Stoof, L. P. H. de Goey, B. J. Verhaar, and W. Glöckle, *Phys. Rev. B* **38**, 11221 (1988).
- [17] B. Statt, Ph.D. thesis, University of British Columbia, Vancouver, 1984.
- [18] S. Vasilyev, J. Järvinen, A. I. Safonov, A. A. Kharitonov, I. I. Lukashevich, and S. Jaakkola, *Phys. Rev. Lett.* **89**, 153002 (2002).
- [19] A. P. Mosk (private communication).
- [20] A. I. Safonov, S. A. Vasilyev, A. A. Kharitonov, S. T. Boldarev, I. I. Lukashevich, and S. Jaakkola, *Phys. Rev. Lett.* **86**, 3356 (2001).
- [21] M. W. Reynolds, I. D. Setija, and G. V. Shlyapnikov, *Phys. Rev. B* **46**, 575 (1992).
- [22] S. A. Vasilyev, E. Tjukanov, M. Mertig, A. Y. Katunin, and S. Jaakkola, *Europhys. Lett.* **24**, 223 (1993).
- [23] H. P. Godfried, E. R. Eliel, J. G. Brisson, J. D. Gillaspay, C. Mallardeau, J. C. Mester, and I. F. Silvera, *Phys. Rev. Lett.* **55**, 1311 (1985).